UiT The Arctic University of Norway

Comparisons of E-region Coherent Scatter Statistics at 49.5 MHz and 32.55 MHz with ICEBEAR and SIMONe Norway

Devin Huyghebaert [1,2], J.L. Chau [3], G. Hussey [2], J.-P. St.-Maurice [2], M.F. Ivarsen [2,4], M. Clahsen [3], R. Latteck [3], T. Renkwitz [3]

(1) UiT The Arctic University of Norway, Tromsø, Norway
(2) University of Saskatchewan, Saskatoon, Canada
(3) Leibniz Institute of Atmospheric Physics, Kühlungsborn, Germany
(4) University of Oslo, Oslo, Norway

DASP 2024, Edmonton, Canada

February 20-23, 2024

Introduction to E-region Plasma Turbulence

(Credit: ESA astronaut Samantha Cristoforetti)
(https://www.nasa.gov/content/aurora-borealis)

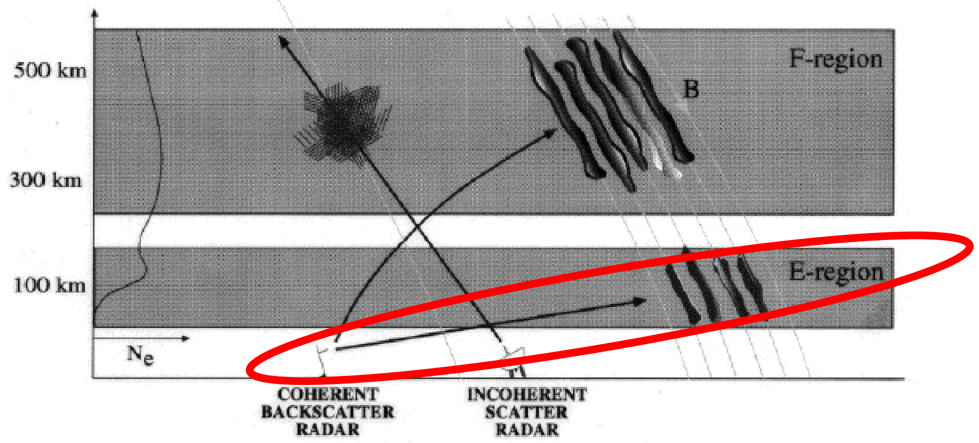

http://vt.superdarn.org/tiki-index.php?page=sd_tutorial

Incoherent vs Coherent Scatter radars

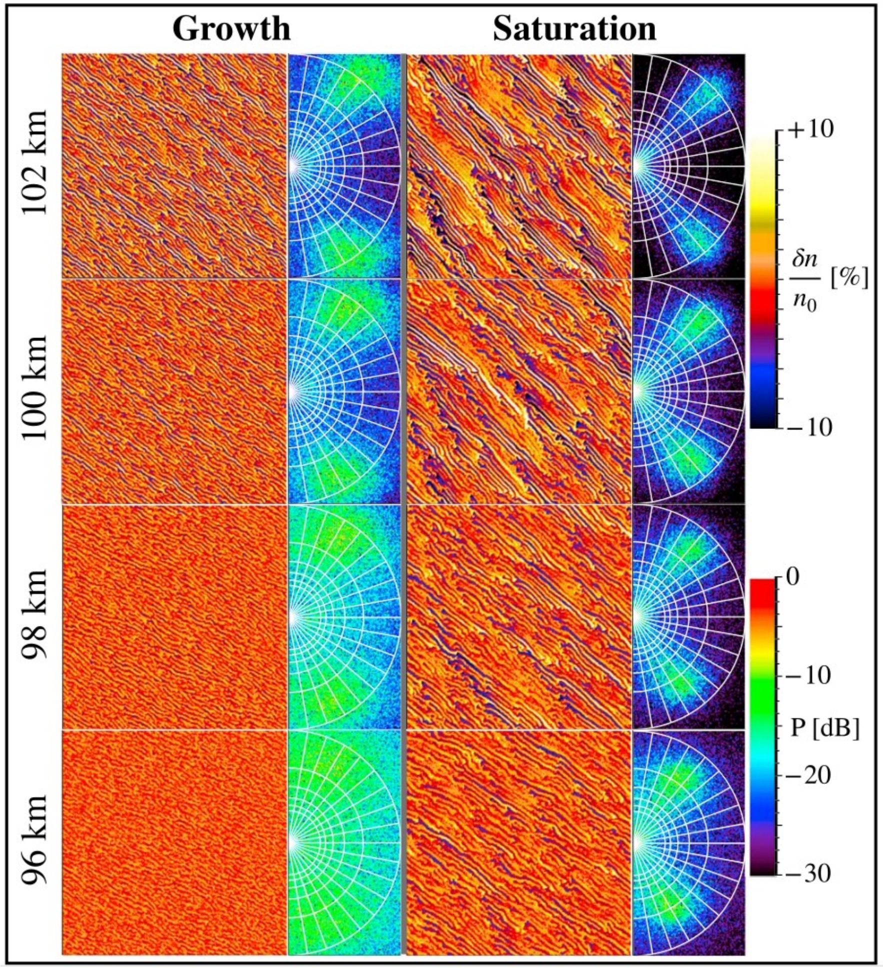

Young, M. A., Oppenheim, M. M., & Dimant, Y. S. (2019). Simulations of secondary Farley-Buneman instability driven by a kilometer-scale primary wave: Anomalous transport and formation of flat-topped electric fields. Journal of Geophysical Research: Space Physics, 124, 734– 748. https://doi.org/10.1029/2018JA026072

The Radar Aurora

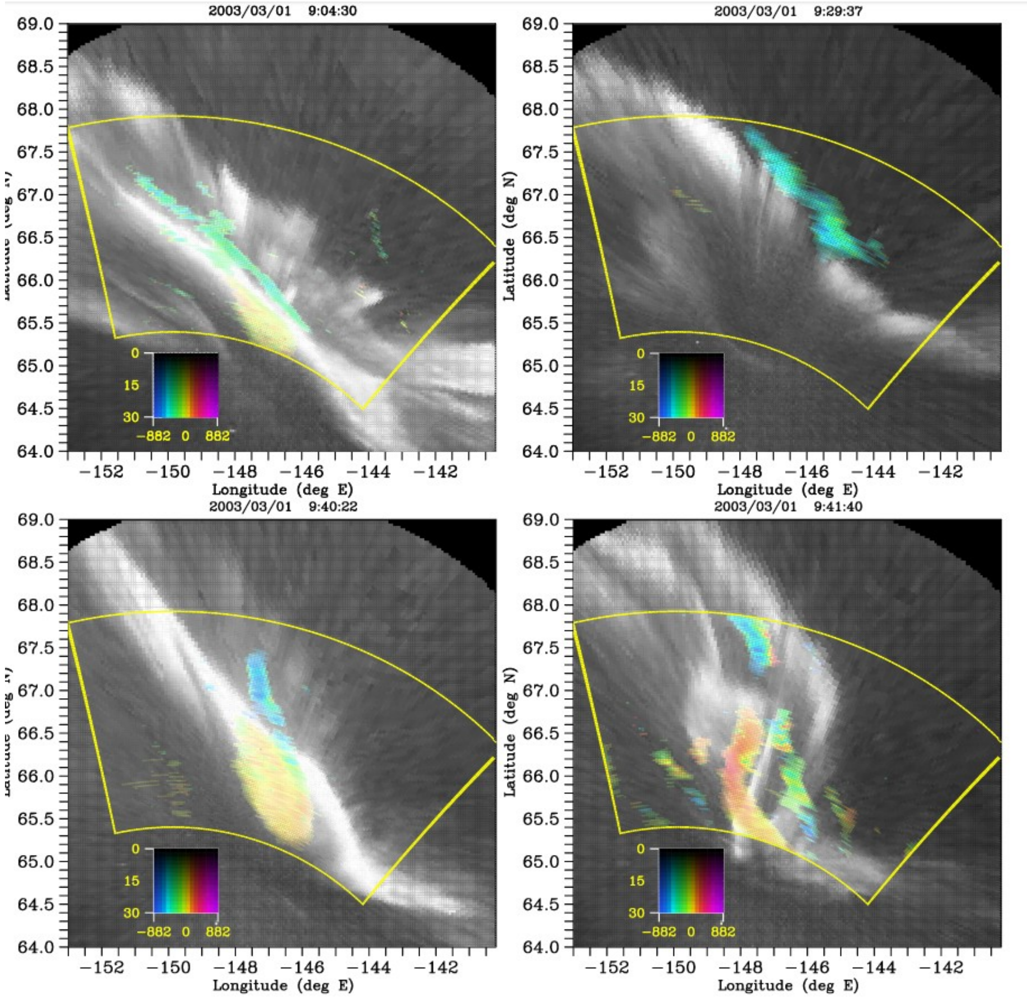

Bahcivan, H., D. L. Hysell, D. Lummerzheim, M. F. Larsen, and R. F. Pfaff (2006), Observations of colocated optical and radar aurora, J. Geophys. Res., 111, A12308, doi:10.1029/2006JA011923.

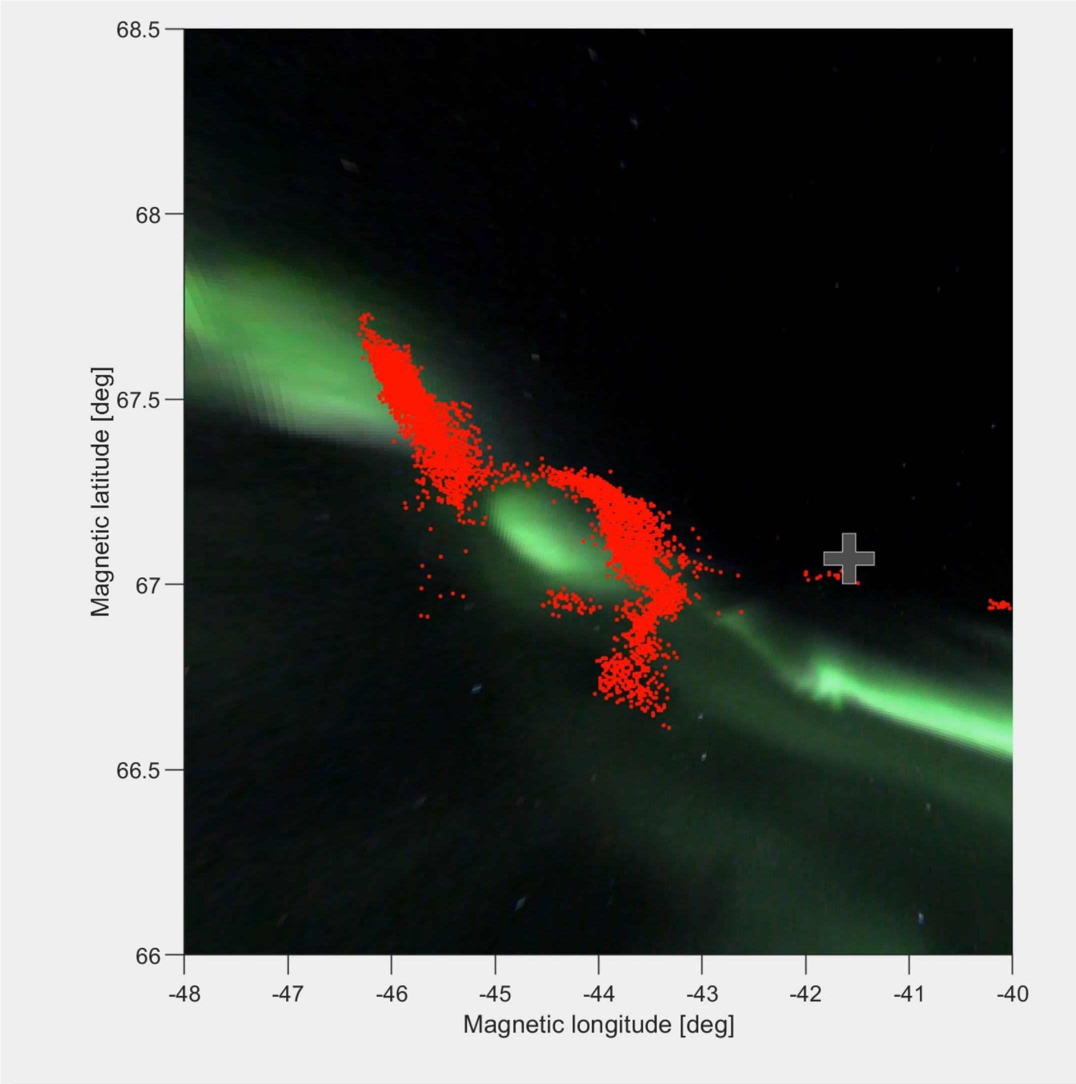

ICEBEAR and TREx
Magnus Ivarsen et al.
Plasma Turbulence Around Auroral Arcs

E-region Coherent Scatter Spectra

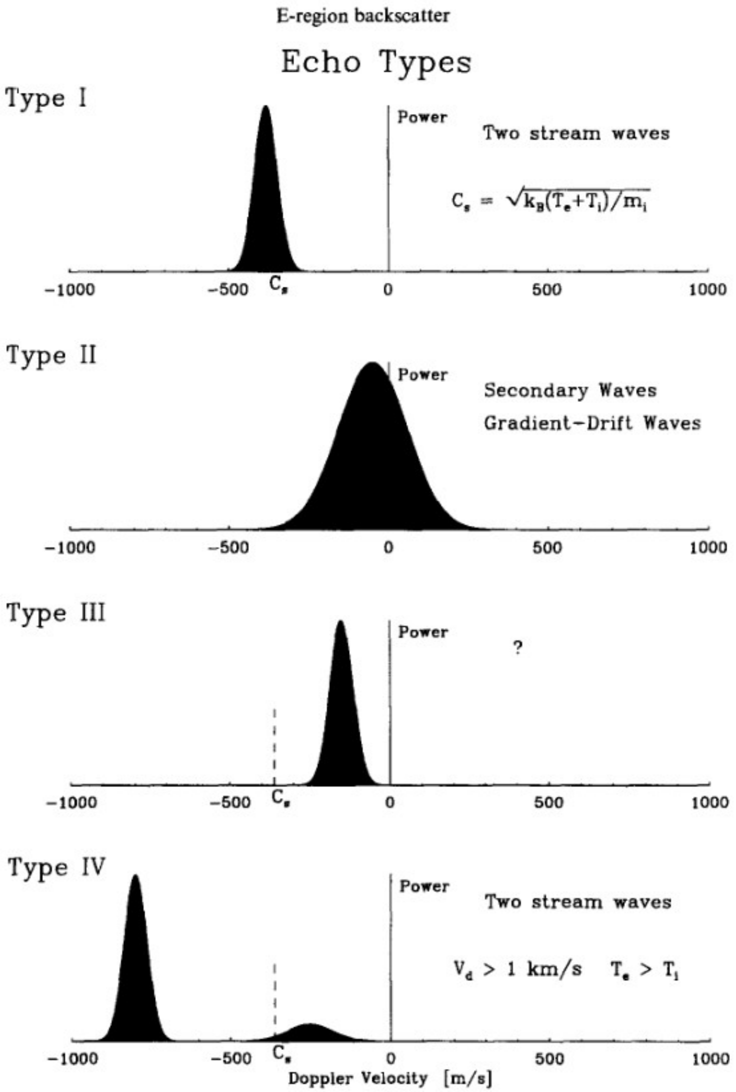

K. Schlegel, Coherent backscatter from ionospheric E-region plasma irregularities, Journal of Atmospheric and Terrestrial Physics, Volume 58, Issues 8–9, 1996, Pages 933-941, ISSN 0021-9169, https://doi.org/10.1016/0021-9169(95)00124-7.

E-region Coherent Scatter Spectra

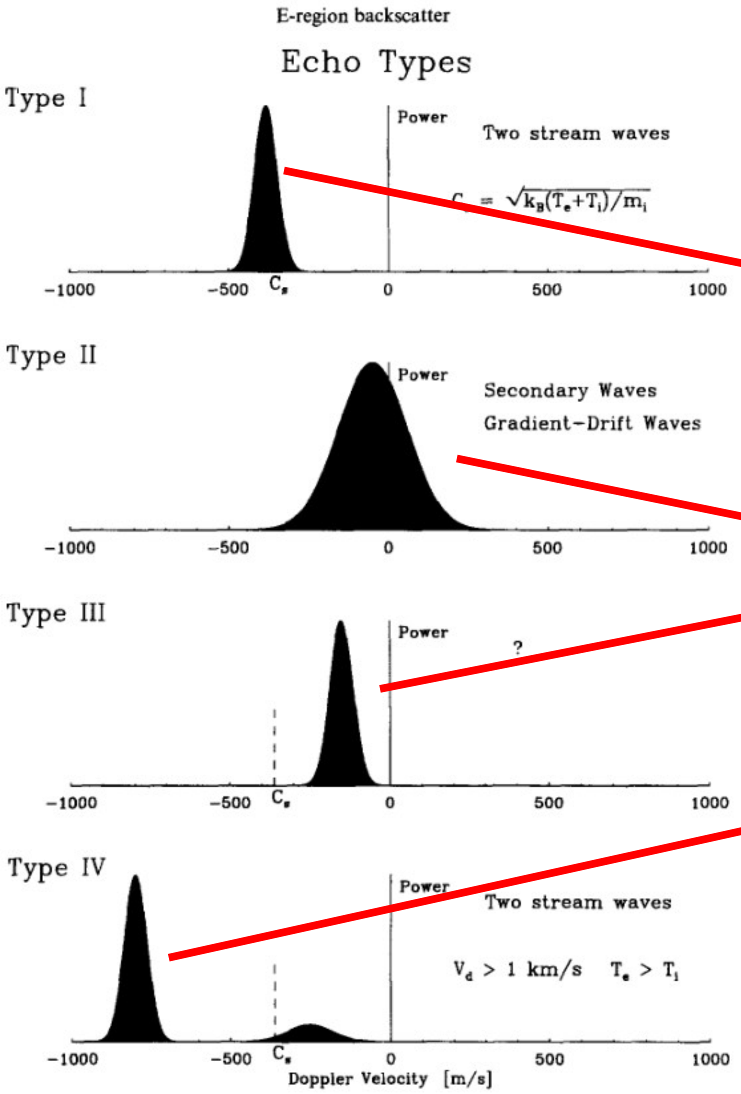

K. Schlegel, Coherent backscatter from ionospheric E-region plasma irregularities, Journal of Atmospheric and Terrestrial Physics, Volume 58, Issues 8–9, 1996, Pages 933-941, ISSN 0021-9169, https://doi.org/10.1016/0021-9169(95)00124-7.

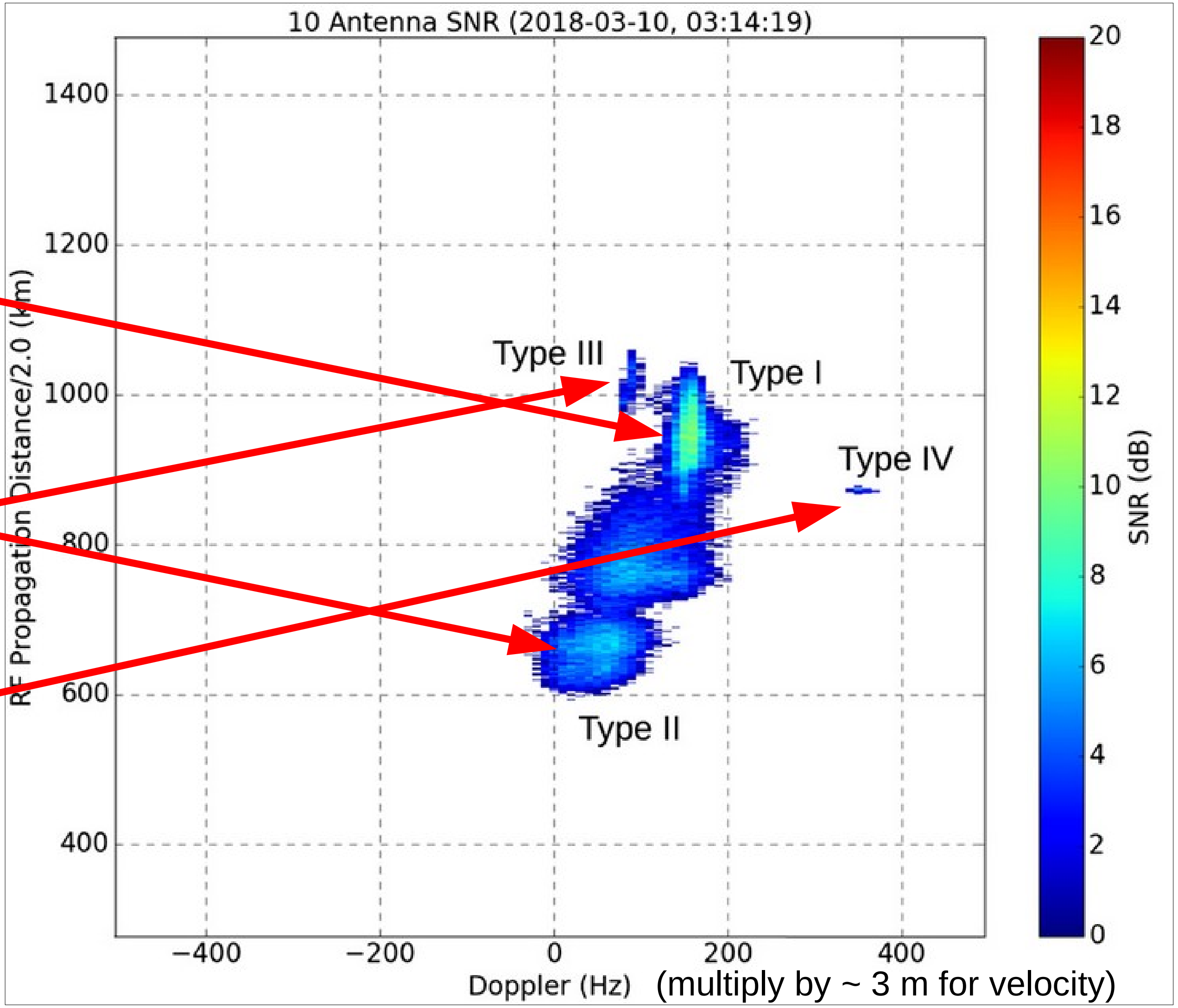

(multiply by ~ 3 m for velocity)

Huyghebaert, D., Hussey, G., Vierinen, J., McWilliams, K., & St.-Maurice, J.-P. (2019). ICEBEAR: An all-digital bistatic coded continuous-wave radar for studies of the E region of the ionosphere. Radio Science, 54, 349–364. https://doi.org/10.1029/2018RS006747

Goal: Electric Field Derivations from E-region Coherent Scatter

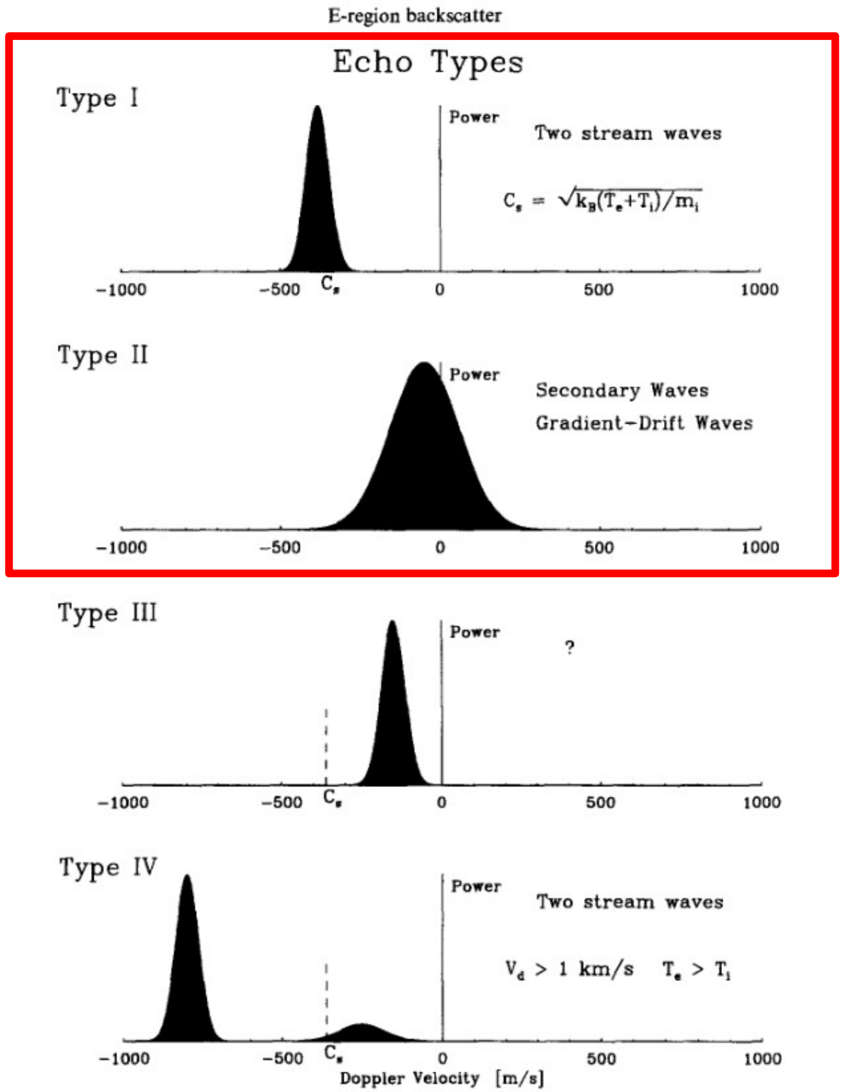

K. Schlegel, Coherent backscatter from ionospheric E-region plasma irregularities, Journal of Atmospheric and Terrestrial Physics, Volume 58, Issues 8–9, 1996, Pages 933-941, ISSN 0021-9169, https://doi.org/10.1016/0021-9169(95)00124-7.

Empirical E-field: Angular dependence of Doppler shift and spectral width with respect to flow angle

Doppler

$$\langle \omega / k \rangle = V_\circ \cos(\theta - \theta_\circ) + v_i$$

Spectral width

$$\langle \delta\omega / k \rangle_{\text{rms}} = \frac{1}{2} V_\circ |\sin(\theta - \theta_\circ)|$$

$$V_\circ = 350 + (V_d/100)^2$$

Hysell, D., R. Miceli, J. Munk, D. Hampton, C. Heinselman, M. Nicolls, S. Powell, K. Lynch, and M. Lessard (2012), Comparing VHF coherent scatter from the radar aurora with incoherent scatter and all-sky auroral imagery, J. Geophys. Res., 117, A10313, doi: 10.1029/2012JA018010.

Rojas, E. L., Hysell, D. L., & Munk, J. (2018). Assessing ionospheric convection estimates from coherent scatter from the radio aurora. Radio Science, 53, 1481–1491. https://doi.org/10.1029/2018RS006672

Goal: Electric Field Derivations from E-region Coherent Scatter

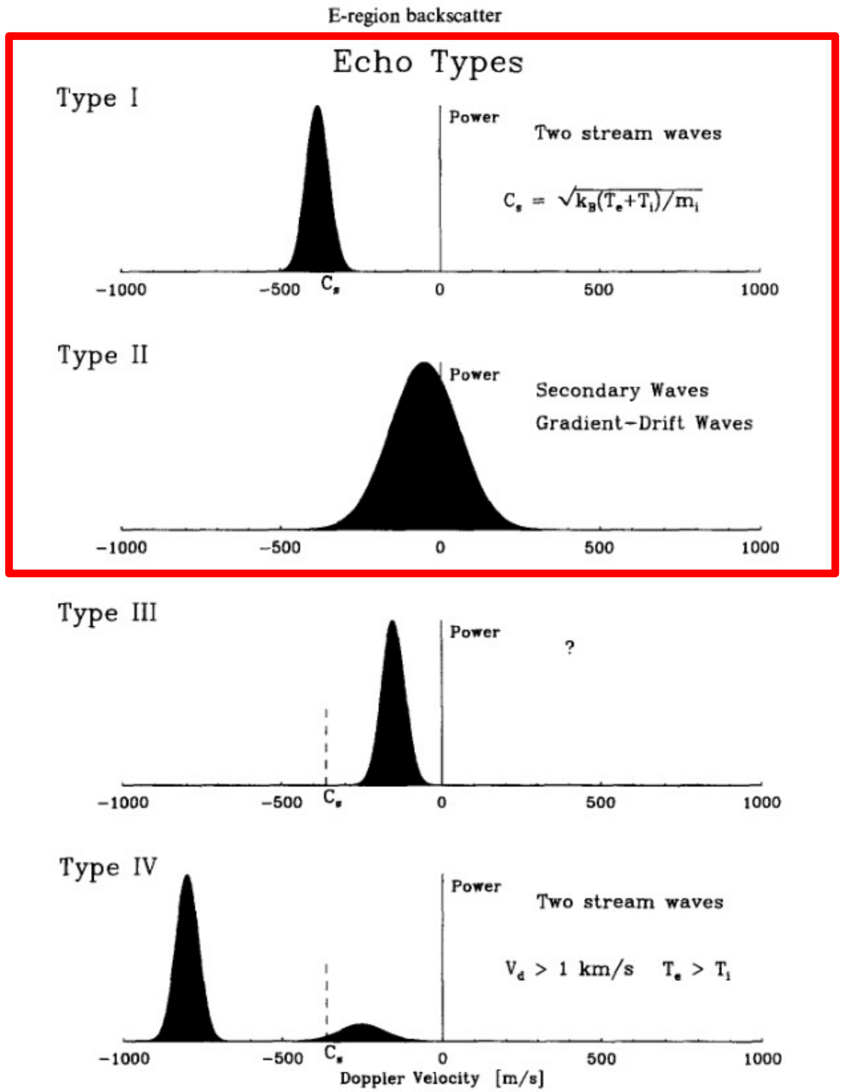

K. Schlegel, Coherent backscatter from ionospheric E-region plasma irregularities, Journal of Atmospheric and Terrestrial Physics, Volume 58, Issues 8–9, 1996, Pages 933-941, ISSN 0021-9169, https://doi.org/10.1016/0021-9169(95)00124-7.

Empirical E-field:
Angular dependence of Doppler shift and spectral width with respect to flow angle

Doppler

$$\langle \omega/k \rangle = V_\circ \cos(\theta - \theta_\circ) + v_i$$

Spectral width

$$\langle \delta\omega/k \rangle_{\mathrm{rms}} = \frac{1}{2} V_\circ |\sin(\theta - \theta_\circ)|$$

$$V_\circ = 350 + (V_d/100)^2$$

System is much more complex

...man, M. Nicolls, S. Powell, K. ... ent scatter from the radar aurora with incoherent scatter and all-sky auroral imagery, J. Geophys. Res., 117, A10313, doi: ...10.

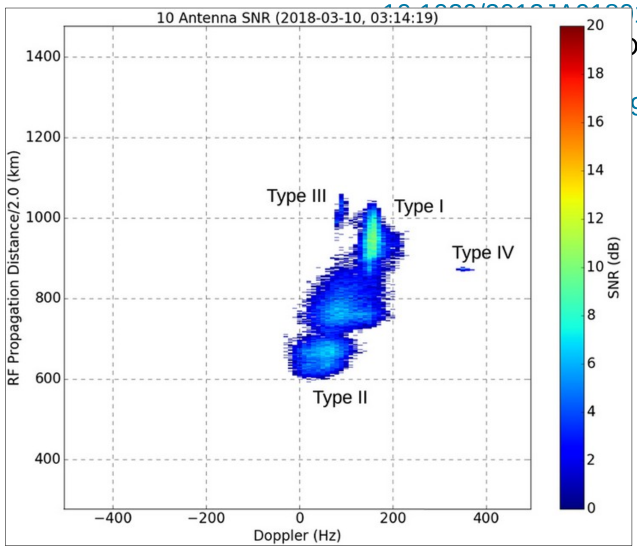

Huyghebaert, D., Hussey, G., Vierinen, J., McWilliams, K., & St.-Maurice, J.-P. (2019). ICEBEAR: An all-digital bistatic coded continuous-wave radar for studies of the E region of the ionosphere. Radio Science, 54, 349–364. https://doi.org/10.1029/2018RS006747

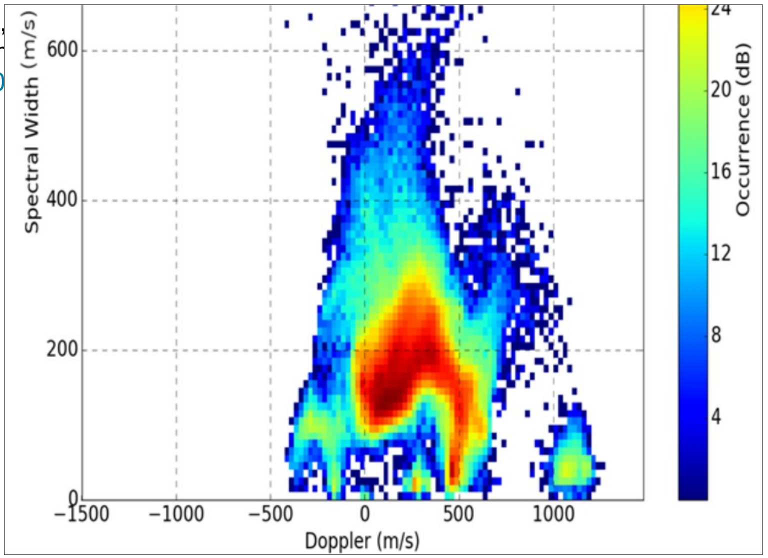

St-Maurice, J.-P., Huyghebaert, D., Ivarsen, M. F., & Hussey, G. C. (2023). Narrow width Farley-Buneman spectra above 100 km altitude. Journal of Geophysical Research: Space Physics, 128, e2022JA031191. https://doi.org/10.1029/2022JA031191

49.5 MHz E-region Coherent Scatter Radar

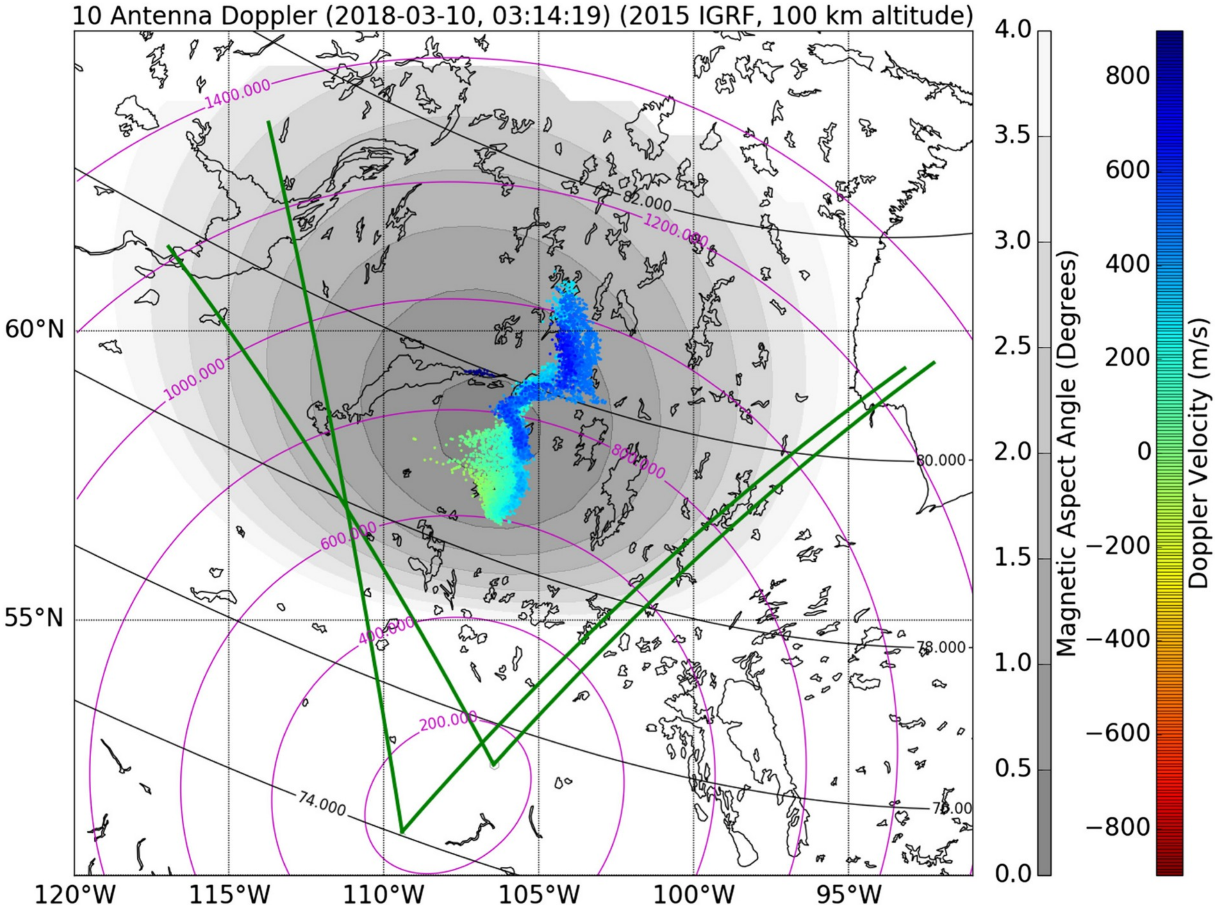

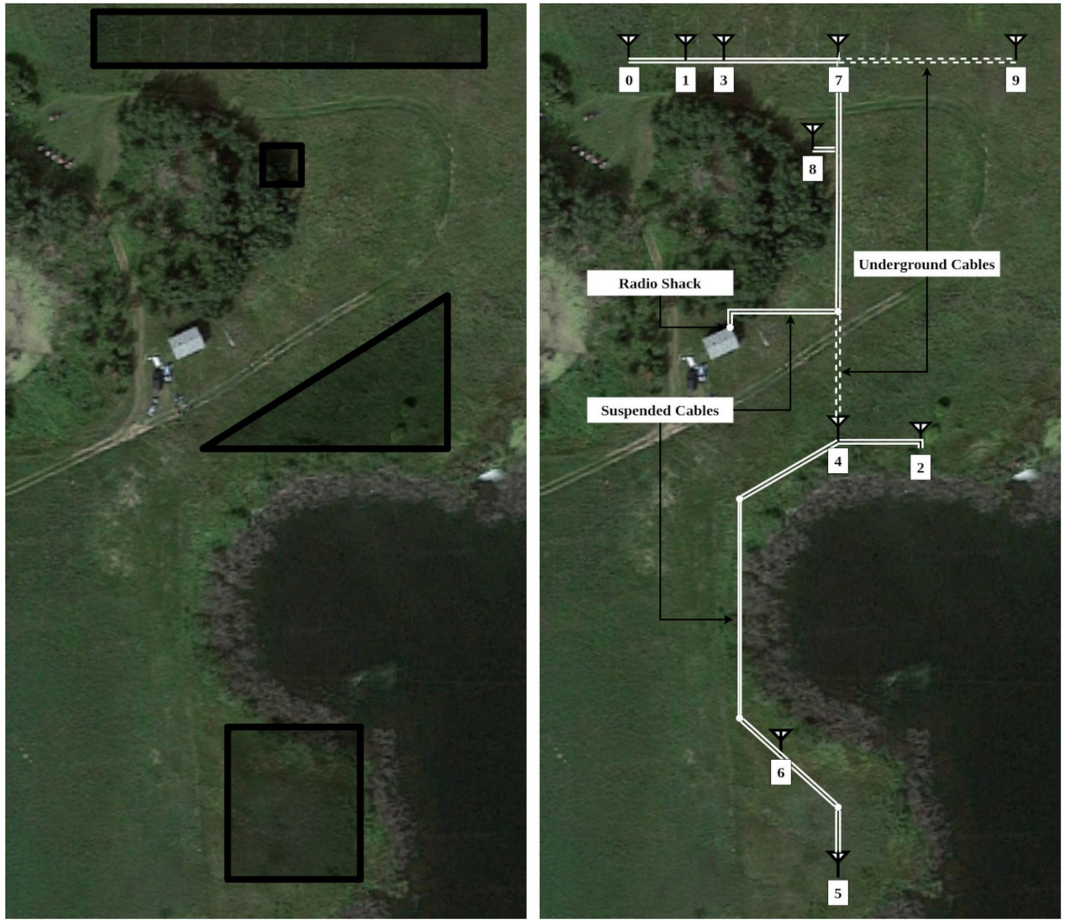

Huyghebaert, D., Hussey, G., Vierinen, J., McWilliams, K., & St.-Maurice, J.-P. (2019). ICEBEAR: An all-digital bistatic coded continuous-wave radar for studies of the E region of the ionosphere. Radio Science, 54, 349–364. https://doi.org/10.1029/2018RS006747

Lozinsky, A., Hussey, G., McWilliams, K., Huyghebaert, D., & Galeschuk, D. (2022). ICEBEAR-3D: A low elevation imaging radar using a non-uniform coplanar receiver array for E region observations. Radio Science, 57, e2021RS007358. https://doi.org/10.1029/2021RS007358

SIMONe Norway Radar System

32.55 MHz Specular Meteor Trail Radar System that can make E-region Coherent Scatter Measurements

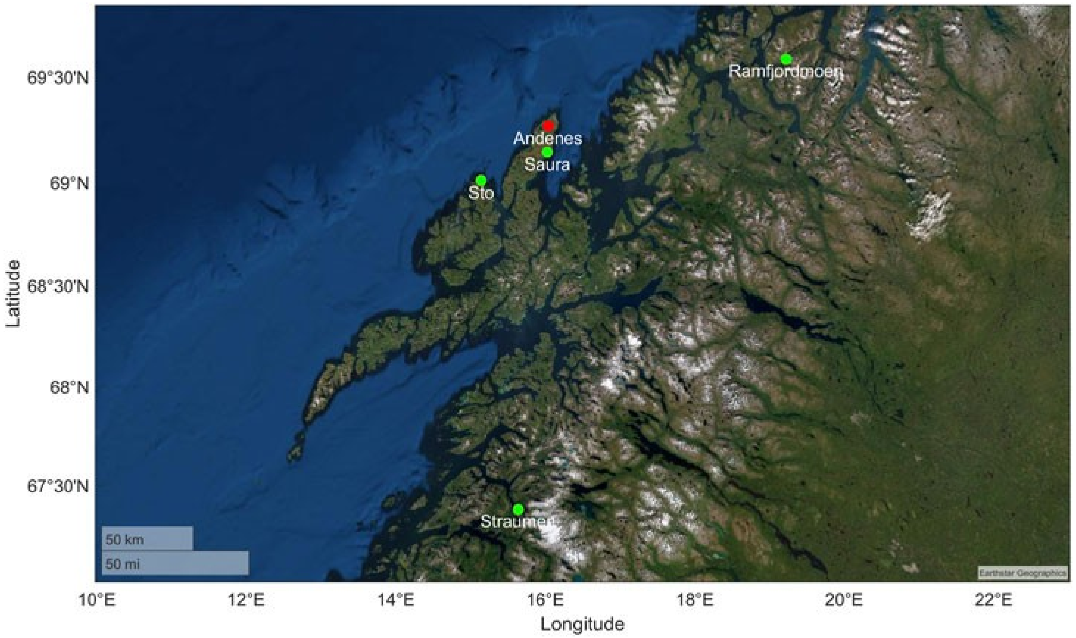

Huyghebaert D, Clahsen M, Chau JL, Renkwitz T, Latteck R, Johnsen MG and Vierinen J (2022) Multiple E-Region Radar Propagation Modes Measured by the VHF SIMONe Norway System During Active Ionospheric Conditions. Front. Astron. Space Sci. 9:886037. doi: 10.3389/fspas.2022.886037

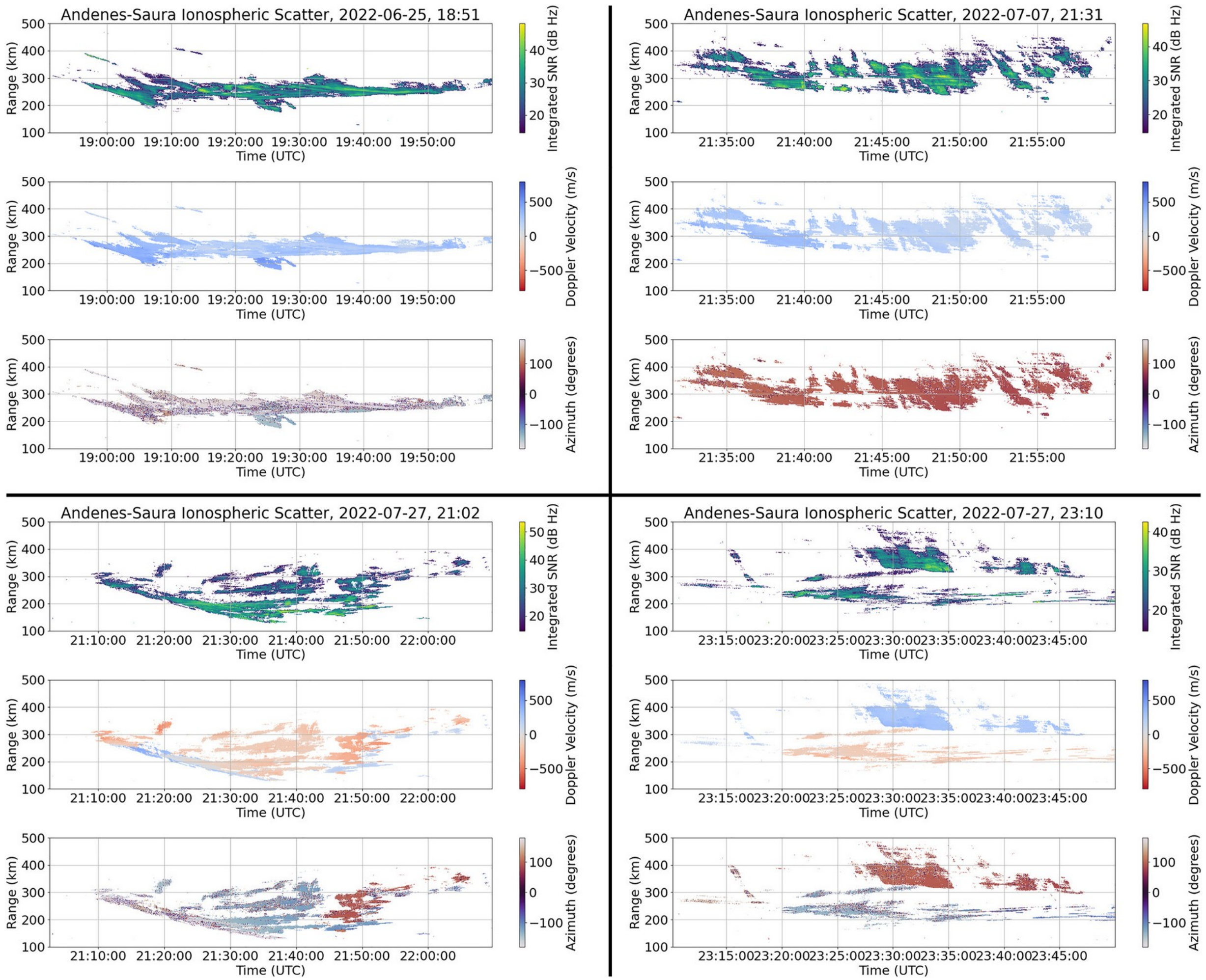

Key Differences between Systems:
- Radar operating frequency
- Scattering geometry

Huyghebaert, D., Chau, J. L., Spicher, A., Ivarsen, M. F., Clahsen, M., Latteck, R., & Vierinen, J. (2023). Investigating spatial and temporal structuring of E-region coherent scattering regions over northern Norway. Journal of Geophysical Research: Space Physics, 128, e2023JA031682. https://doi.org/10.1029/2023JA031682

ICEBEAR and SIMONe Spectral Widths

> 10 dB SNR threshold

Significant amount more ICEBEAR than SIMONe data

- ICEBEAR records and processes coherent scatter every evening

- SIMONe data recorded for E-region coherent scatter studies on request

SIMONe Norway not optimized for geomagnetic perpendicular aspect conditions

- main purpose is for meteor trails

- scatter must be due to refracted signal and/or non-aspect sensitive plasma turbulence

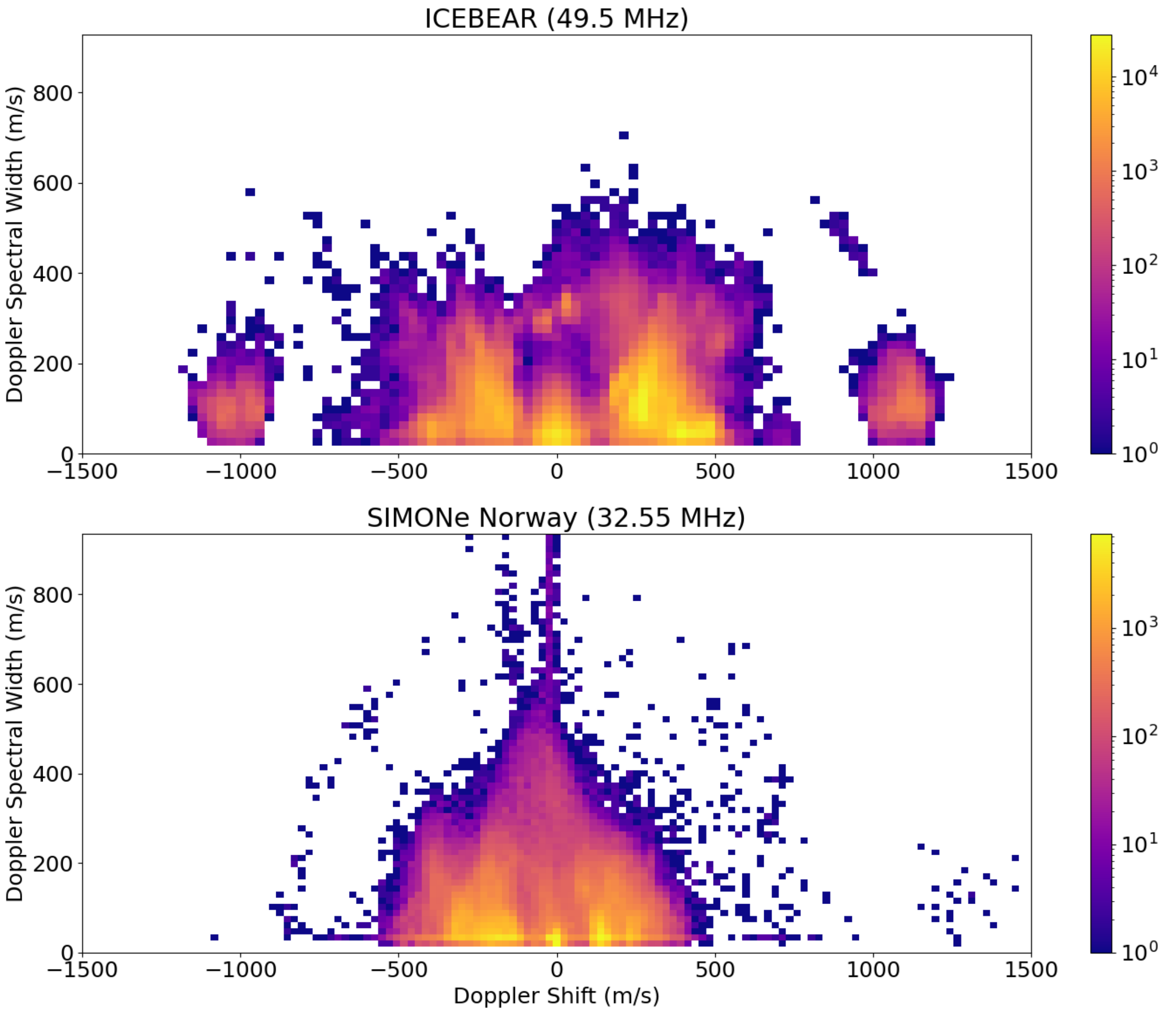

ICEBEAR and SIMONe Spectral Widths

Doppler

$$\langle \omega/k \rangle = V_\circ \cos(\theta - \theta_\circ) + v_i$$

Spectral width

$$\langle \delta\omega/k \rangle_{\text{rms}} = \frac{1}{2} V_\circ |\sin(\theta - \theta_\circ)|$$

$$V_\circ = 350 + (V_d/100)^2$$

Hysell, D., R. Miceli, J. Munk, D. Hampton, C. Heinselman, M. Nicolls, S. Powell, K. Lynch, and M. Lessard (2012), Comparing VHF coherent scatter from the radar aurora with incoherent scatter and all-sky auroral imagery, J. Geophys. Res., 117, A10313, doi: 10.1029/2012JA018010.

Rojas, E. L., Hysell, D. L., & Munk, J. (2018). Assessing ionospheric convection estimates from coherent scatter from the radio aurora. Radio Science, 53, 1481–1491. https://doi.org/10.1029/2018RS006672

Distributions don't follow these expectations

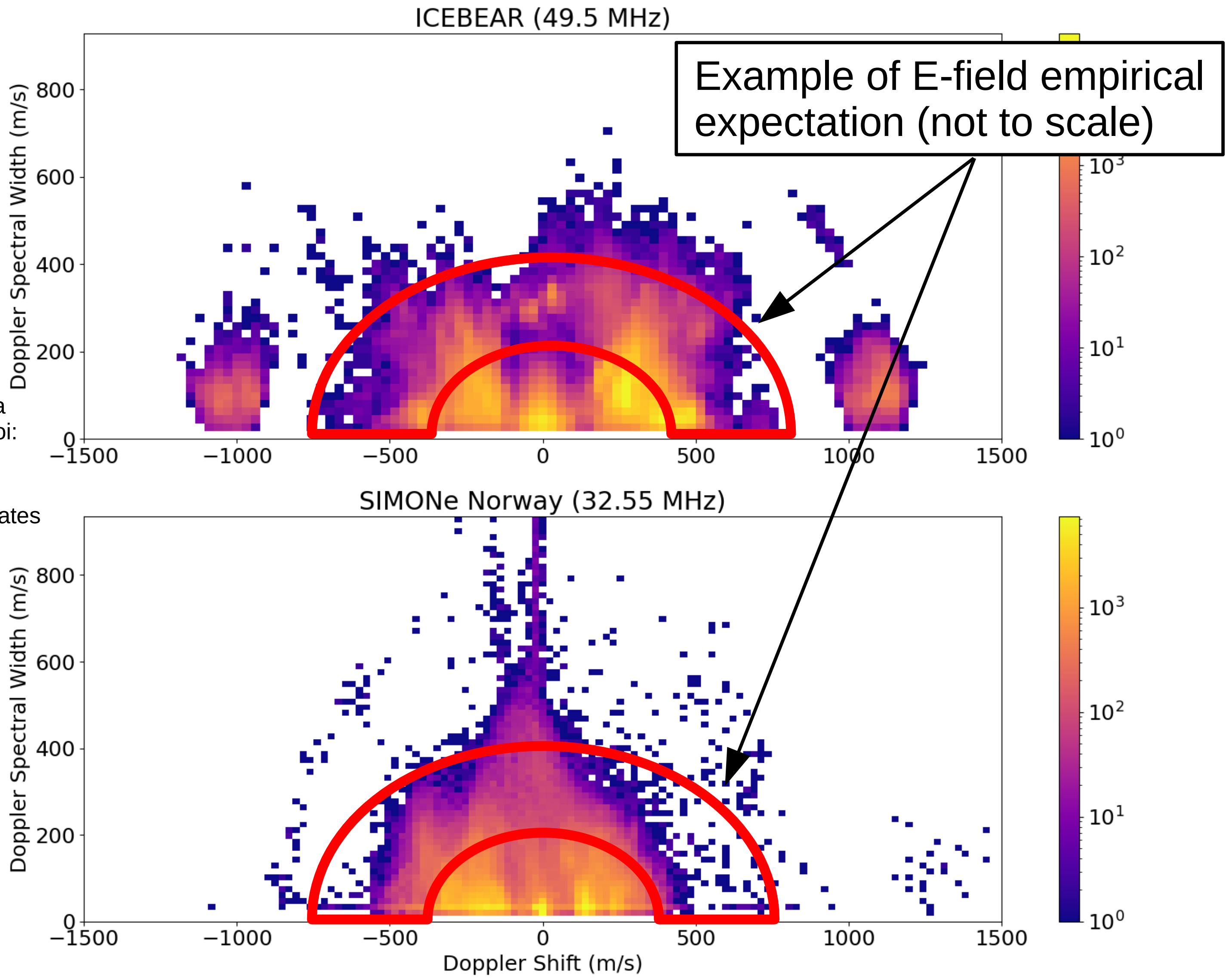

UiT The Arctic University of Norway

ICEBEAR and SIMONe Spectral Widths

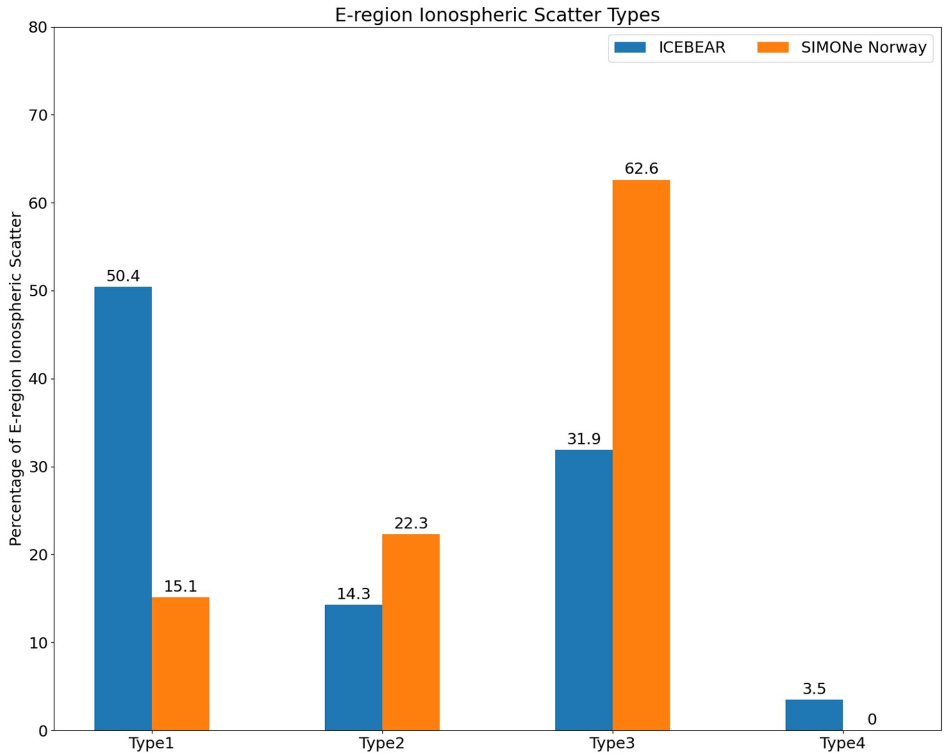

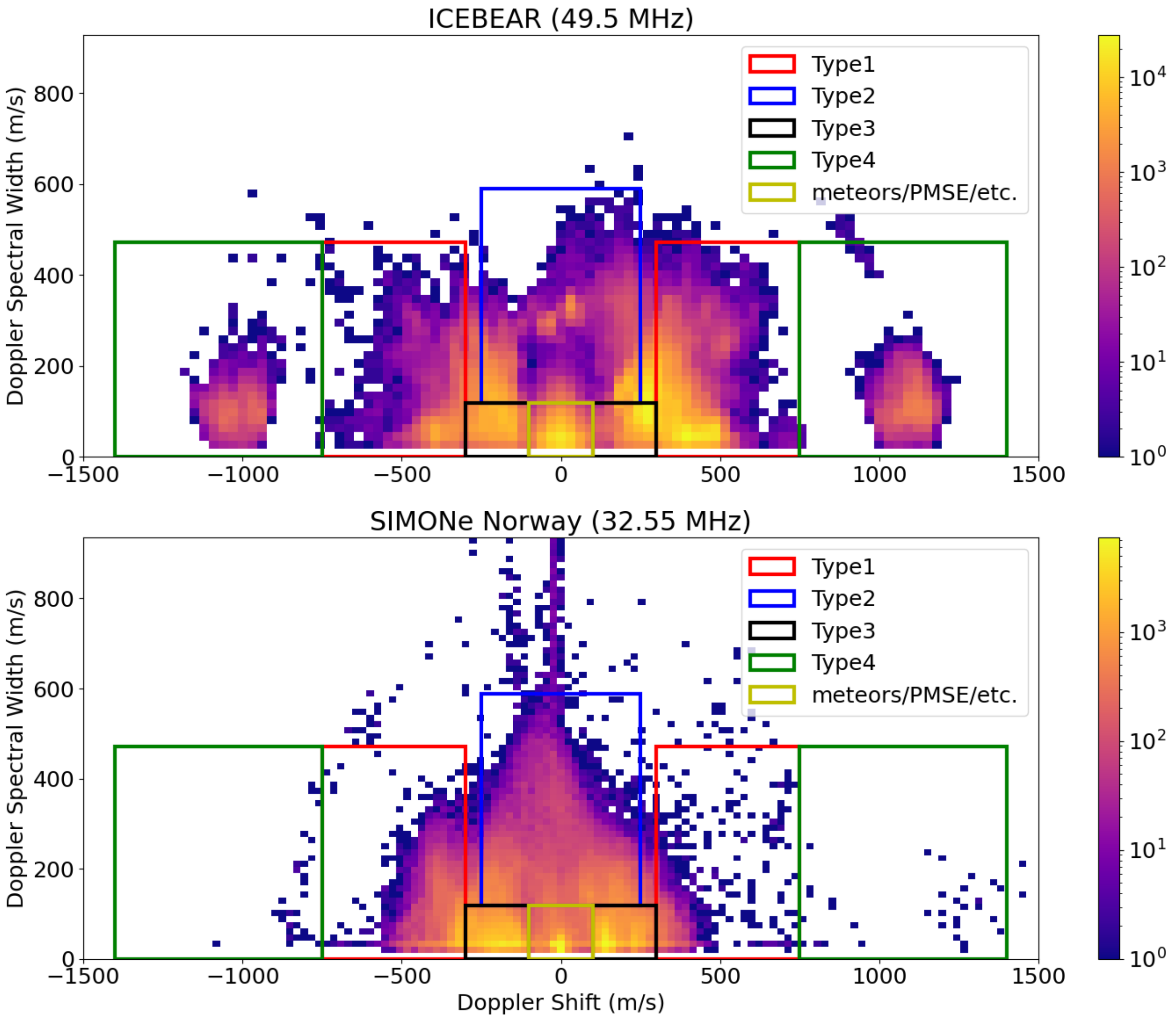

ICEBEAR and SIMONe Spectral Widths

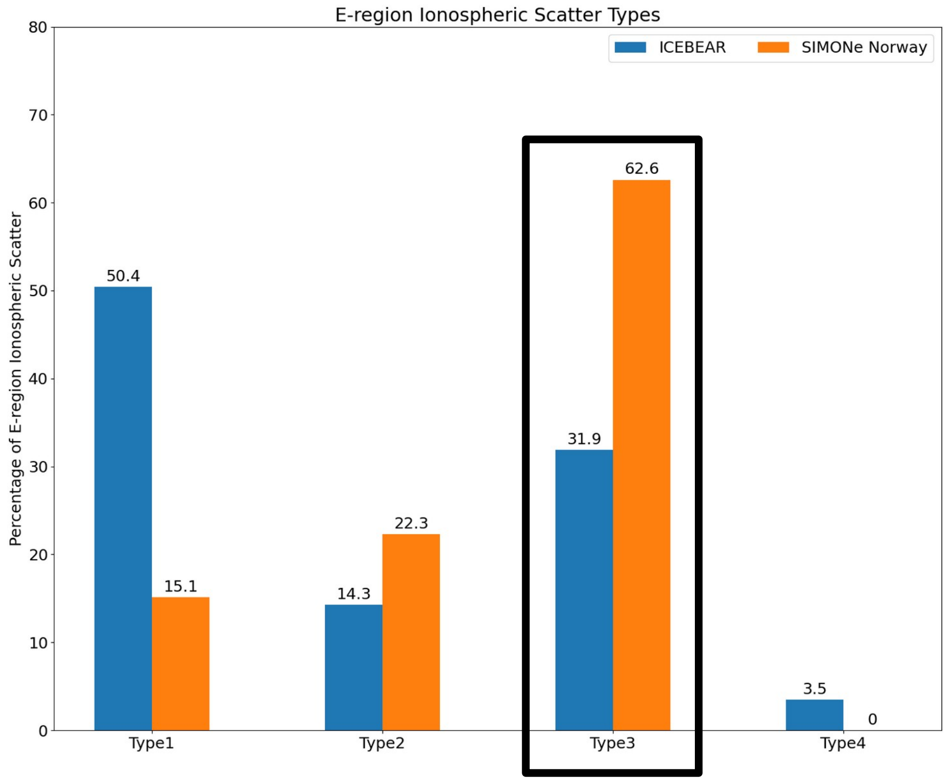

100-300 m/s Doppler Velocity
< 120 m/s Doppler Standard Deviation

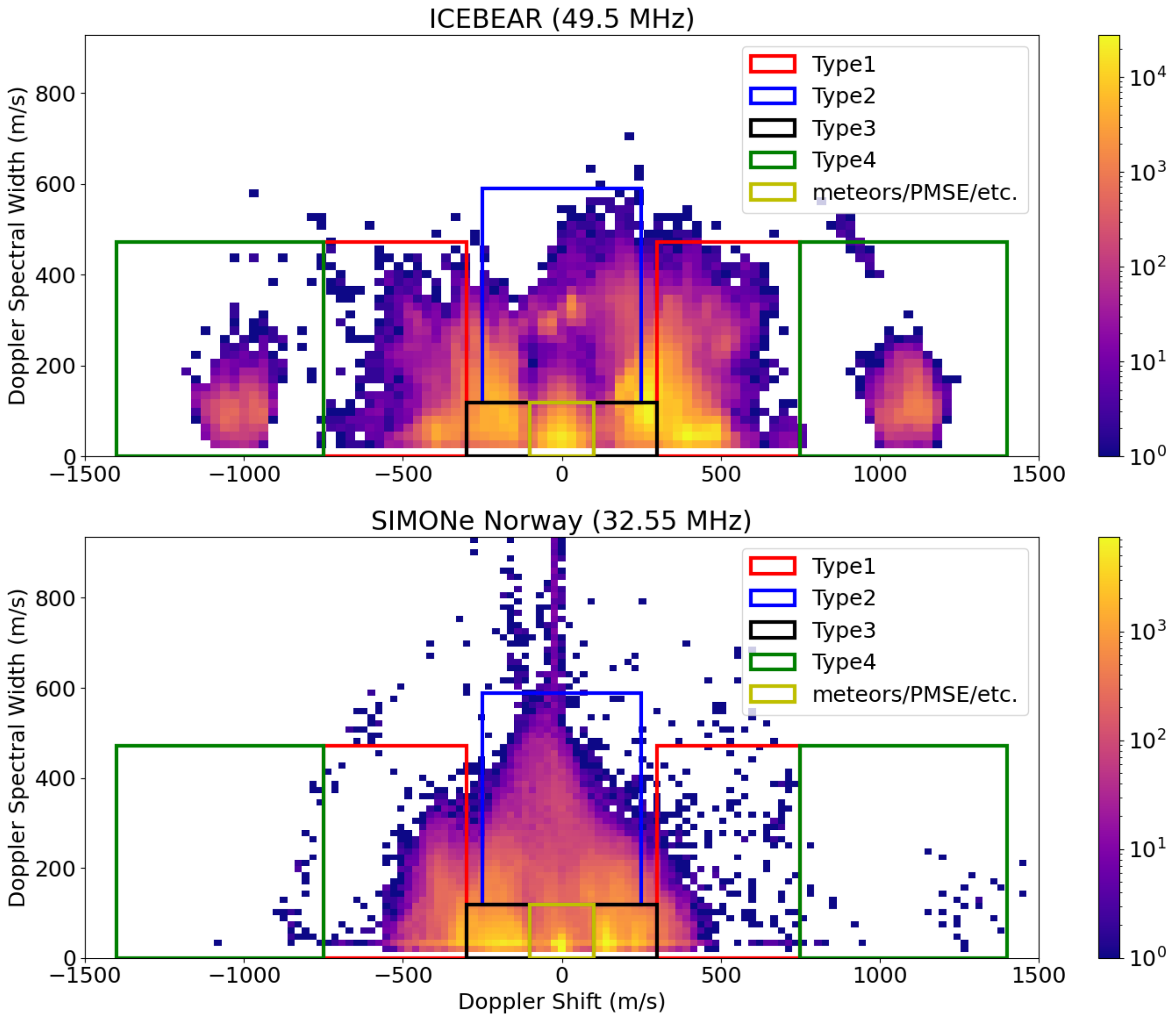

Altitude and Doppler Histograms

Angle of arrival used for altitude w/ ICEBEAR
- extensive interferometer on receive

Angle of departure used for altitude with SIMONe
- coherent Multi-Input Single-Ouput (MISO)
    - transmission of different codes from antennas at the same transmit site

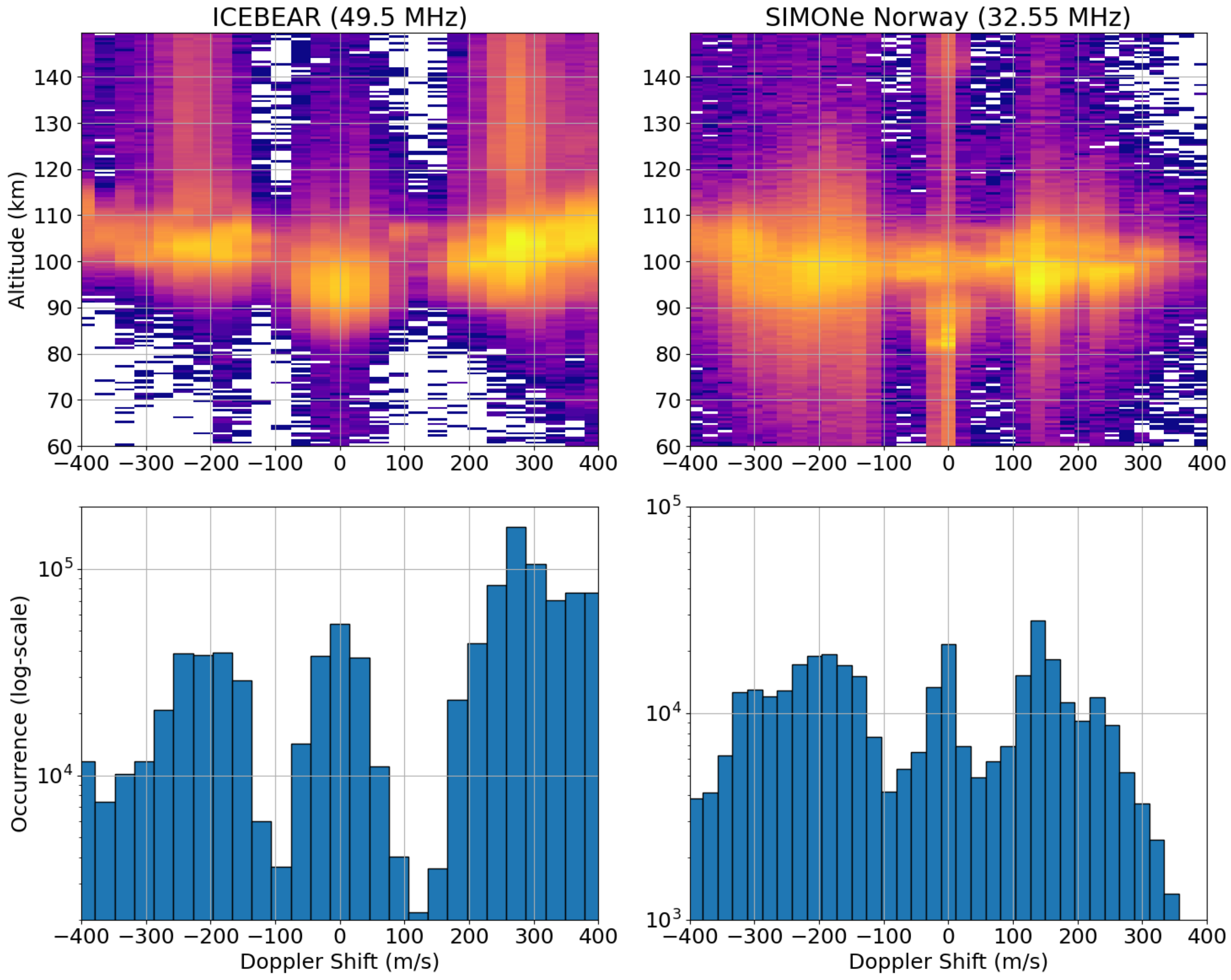

Altitude and Doppler Histograms

Angle of arrival used for altitude w/ ICEBEAR
- extensive interferometer on receive

Angle of departure used for altitude with SIMONe
- coherent Multi-Input Single-Ouput (MISO)
  - transmission of different codes from antennas at the same transmit site

<u>Radar wavelengths:</u>

SIMONe: ~ 9.22 m
ICEBEAR: ~ 6.06 m

Ratio: ~ 1.52

<u>Threshold phase speed:</u>

SIMONe: ~ 115 +/- 12 m/s
ICEBEAR: ~ 151 +/- 15 m/s

Ratio: ~ 0.76
1/Ratio: ~ 1.31

~ 115 m/s

~ 151 m/s

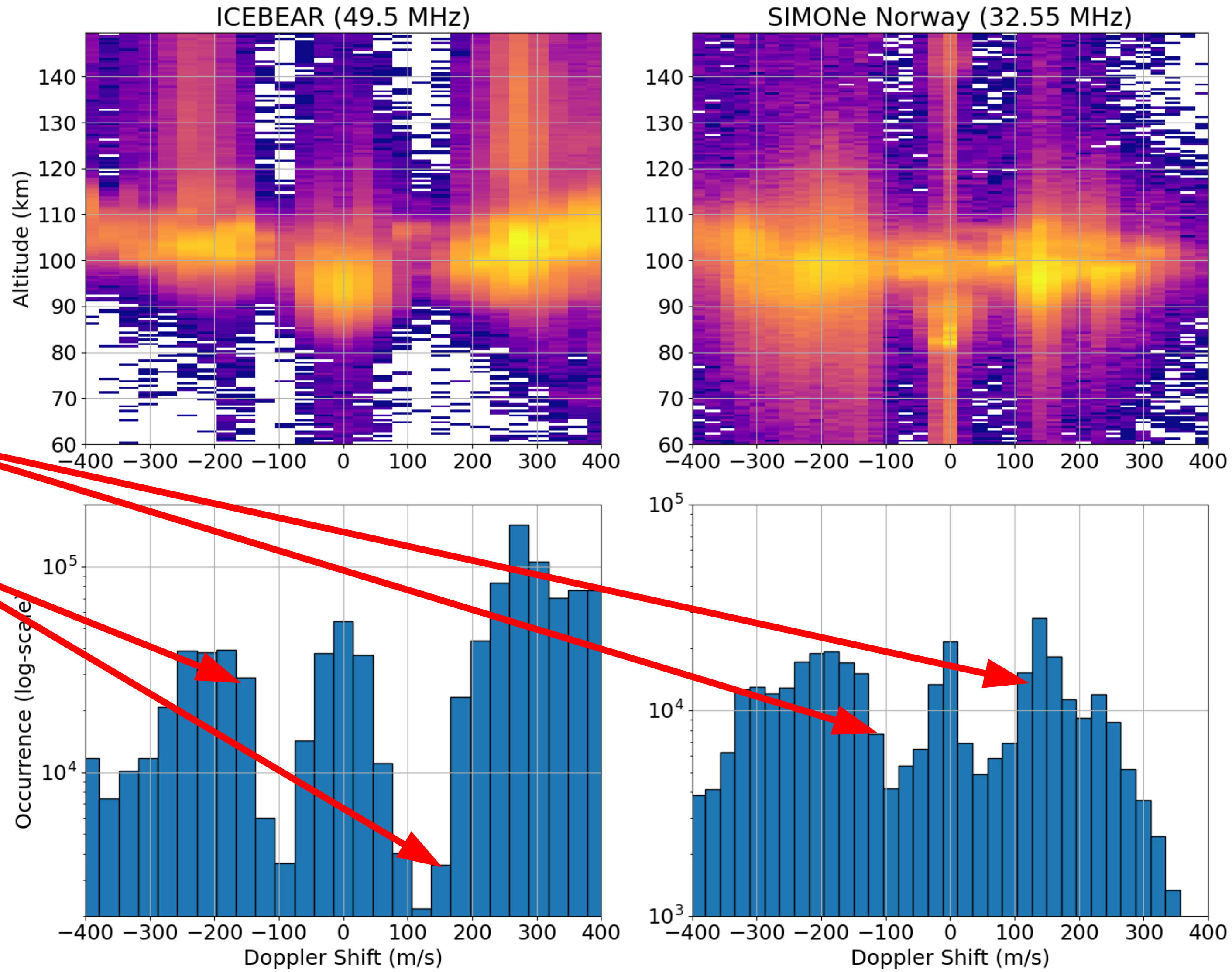

Different Explanations of Type 3 Scatter

MEOHW Mechanism (St.-Maurice and Chau, 2016)

St.-Maurice, J.-P. and J. L. Chau (2016), A theoretical framework for the changing spectral properties of meter-scale Farley-Buneman waves between 90 and 125 km altitudes, J. Geophys. Res. Space Physics, 121, 10,341–10,366, doi:10.1002/2016JA023105.

MIOHW Mechanism (Dimant & Oppenheim, 2004)

Y.S. Dimant, M.M. Oppenheim, Ion thermal effects on E-region instabilities: linear theory, Journal of Atmospheric and Solar-Terrestrial Physics, Volume 66, Issue 17, 2004, Pages 1639-1654, ISSN 1364-6826,https://doi.org/10.1016/j.jastp.2004.07.006.

Ion Motion Contribution (St.-Maurice et al., 2023)

St-Maurice, J.-P., Huyghebaert, D., Ivarsen, M. F., & Hussey, G. C. (2023). Narrow width Farley-Buneman spectra above 100 km altitude. Journal of Geophysical Research: Space Physics, 128, e2022JA031191. https://doi.org/10.1029/2022JA031191

Plasma Density Gradient (St.-Maurice et al., 1994)

St.-Maurice, J.-P., P. Prikryl, D. W. Danskin, A. M. Hamza, G. J. Sofko, J. A. Koehler, A. Kustov, and J. Chen (1994), On the origin of narrow non-ion-acoustic coherent radar spectra in the high-latitude E region, J. Geophys. Res., 99(A4), 6447–6474, doi:10.1029/93JA02353.

Aspect Angle Effects (Foster et al. 1992)

Foster, J. C., D. Tetenbaum, C. F. delPozo, J.-P. St-Maurice, and D. R. Moorcroft (1992), Aspect angle variations in intensity, phase velocity, and altitude for high-latitude 34-cm E region irregularities, J. Geophys. Res., 97(A6), 8601–8617, doi:10.1029/91JA03144.

Characteristics to Further Consider for ‘Type 3’

Is there a less restrictive aspect angle dependence for the narrow, slow scatter?

Is altitude less of a factor than typical Farley-Buneman turbulence for narrow, slow scatter?

Is there a difference in phase speed threshold for the instability at different radar wavelengths?

The ‘Type 3’ spectra still do not occur in the brightest regions of the aurora.
Is this an electric field effect, a plasma gradient effect, or a combination of the two?

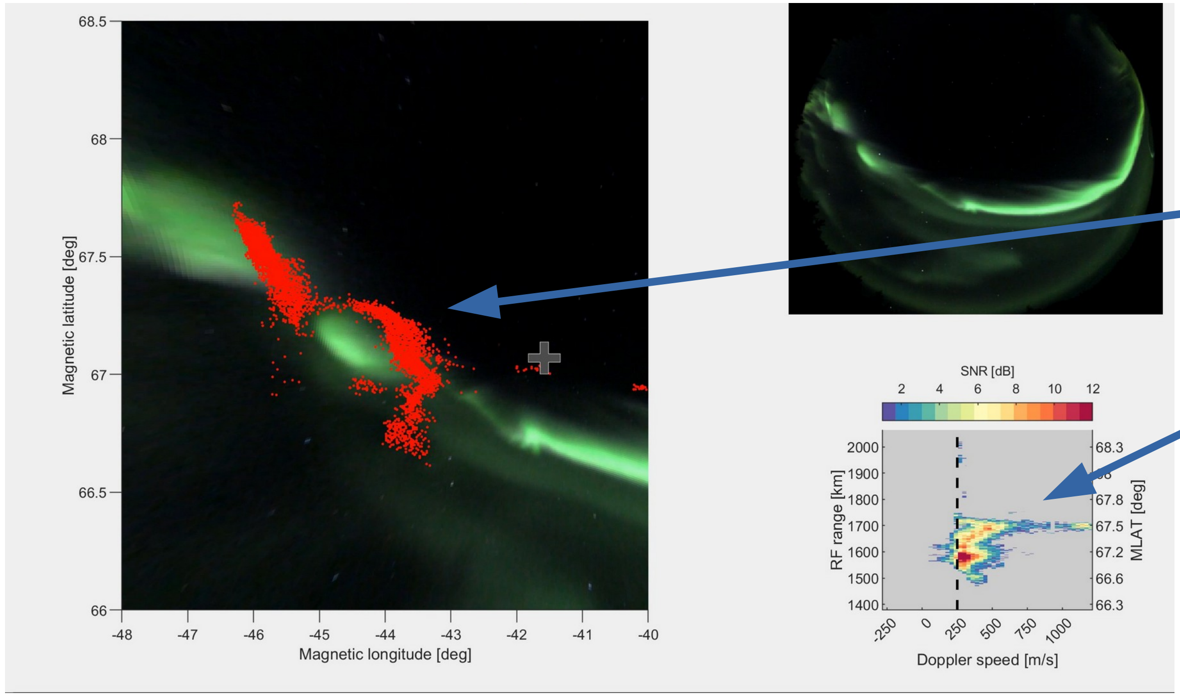

Goal is to obtain high accuracy electric field data from E-region radar spectra in these regions

ICEBEAR and TREx
Magnus Ivarsen et al.
Plasma Turbulence Around Auroral Arcs

Questions?

The Research Council of Norway

UiT The Arctic University of Norway

LEIBNIZ INSTITUTE OF ATMOSPHERIC PHYSICS IAP

DFG

NSERC CRSNG

CSA ASC

innovation SASKATCHEWAN

UNIVERSITY OF SASKATCHEWAN

INNOVATION.CA
CANADA FOUNDATION FOR INNOVATION | FONDATION CANADIENNE POUR L'INNOVATION

devin.r.huyghebaert@uit.no

Summary

- E-region coherent scatter requires a combination of plasma density and large electric fields

Williams, P. J. S., Jones, B., Kustov, A. V., and Uspensky, M. V. (1999), The relationship between E region electron density and the power of auroral coherent echoes at 45 MHz, Radio Sci., 34(2), 449– 457, doi:10.1029/1998RS900039.

Huyghebaert, D., St.-Maurice, J.-P., McWilliams, K., Hussey, G., Howarth, A. D., Rutledge, P., & Erion, S. (2021). The properties of ICEBEAR E-region coherent radar echoes in the presence of near infrared auroral emissions, as measured by the Swarm-E fast auroral imager. Journal of Geophysical Research: Space Physics, 126. https://doi.org/10.1029/2021JA029857

- The scatter can be used as a tracer for field-aligned currents

Ivarsen, M. F., Lozinsky, A., St-Maurice, J.-P., Spicher, A., Huyghebaert, D., Hussey, G. C., et al. (2023). The distribution of small-scale irregularities in the E-region, and its tendency to match the spectrum of field-aligned current structures in the F-region. Journal of Geophysical Research: Space Physics, 128, e2022JA031233. https://doi.org/10.1029/2022JA031233

- The scatter can be used to determine structuring of ionospheric and magnetospheric processes

Ivarsen, M. F., Lozinsky, A., St-Maurice, J.-P., Spicher, A., Huyghebaert, D., Hussey, G. C., et al. (2023). The distribution of small-scale irregularities in the E-region, and its tendency to match the spectrum of field-aligned current structures in the F-region. Journal of Geophysical Research: Space Physics, 128, e2022JA031233. https://doi.org/10.1029/2022JA031233

Huyghebaert, D., Chau, J. L., Spicher, A., Ivarsen, M. F., Clahsen, M., Latteck, R., & Vierinen, J. (2023). Investigating spatial and temporal structuring of E-region coherent scattering regions over northern Norway. Journal of Geophysical Research: Space Physics, 128, e2023JA031682. https://doi.org/10.1029/2023JA031682

- Obtaining accurate electric fields at km-scales from coherent scatter is difficult
    - Ambiguity due to refraction, diversity of spectra and instabilities

- Still existing questions surrounding Type 3 E-region coherent scatter:
    - Does it actually have a large altitude range of occurrence?
    - Is there a wavelength dependence on the threshold phase speed for some scatter?
    - Is there a combination of multiple different instability processes with similar spectral characteristics?

Due to the large occurrence of Type-3 scatter, understanding the conditions for the narrow sub-ion-acoustic spectra is one of the final hurdles to making high resolution E-field determinations from E-region coherent scatter